34th Wind Energy Symposium. AIAA paper 2016-1992
Preprint version. DOI: 10.2514/6.2016-1992

Measuring power output intermittency and unsteady loading in a micro wind farm model

Juliaan Bossuyt*
KU Leuven, Leuven, B3001, Belgium

Charles Meneveau†
Johns Hopkins University, Baltimore, Maryland, MD 21218, USA

Johan Meyers‡
KU Leuven, Leuven, B3001, Belgium

In this study porous disc models are used as a wind turbine model for a wind-tunnel wind farm experiment, allowing the measurement of the power output, thrust force and spatially averaged incoming velocity for every turbine. The model's capabilities for studying the unsteady turbine loading, wind farm power output intermittency and spatio temporal correlations between wind turbines are demonstrated on an aligned wind farm, consisting of 100 wind turbine models.

I. Introduction

Power output intermittency introduces a challenge for the integration of wind farms in electric power grids. Fluctuations in the power output originate from the turbulent nature of the atmospheric boundary layer, further complicated by wind turbine wake interactions. The corresponding unsteady loading directly influences the wind turbine lifetime. Detailed information about the spectrum of the power output is necessary to define the ancillary power generation units needed to provide the required fill-in power when a power signal from the grid operator has to be tracked.[1] Power output intermittency and turbine unsteady loading can thus be considered as an important factor in the energy cost of wind farms. Minimizing these unwanted phenomena can be done by finding an optimal wind farm layout[2,3] or by making use of active wind turbine control.[4,5] This requires detailed spatio-temporal information about the power output and turbine loading for the entire wind farm. From LES data it was found that the power outputs of streamwise aligned wind turbines show a significant correlation.[6] It has also been found, based on LES[6] and field data[1] , that the spectrum of the total power output of a wind farm seems to follow a Kolmogorov power law. However, based on a detailed analysis and comparisons with field data, the origins for this $-5/3$ power law and their connection to the wind farm layout and atmospheric boundary layer characteristics still form an open question.[1,6] Due to difficulties with flow similarity, experimental studies of large wind farms typically focus on mean row power and boundary layer flow characteristics[7–14] , while lacking this crucial temporal information. In this study we carry out an experimental wind-tunnel study of an aligned wind farm with 100 wind turbine models. By using a specially designed porous disc model we are able to measure the power output, turbine loading and spatially averaged hub velocity with a high enough frequency response to study unsteady loading, power output variability and spatio-temporal correlations in the wind farm.

*Doctoral student, Department of Mechanical Engineering,KU Leuven, Celestijnenlaan 300A, B3001 Leuven, Belgium.
†L.M. Sardella Professor of Mechanical Engineering, Department of Mechanical Engineering and Center for Environmental and Applied Fluid Mechanics, Johns Hopkins University, 3400 North Charles Street, Baltimore, MD21218, USA.
‡Associate Professor, Department of Mechanical Engineering, KU Leuven, Celestijnenlaan 300A, B3001 Leuven, Belgium.

II. Experimental set-up

II.A. Wind turbine model

An experimental wind-tunnel set-up of a large wind turbine array including over 100 turbines requires a very small-scale turbine model. (Figure 1) Simplifying the experimental set-up and focusing on measuring the power output, there are two main requirements for the wind turbine model: the model should have the correct relation between the incoming flow characteristics and the turbine power and it should have the correct wake characteristics in function of the incoming flow.[11] Porous disc models can be used to represent the self similar far wake of a rotating wind turbine in a turbulent flow.[11,15,16] The total thrust force on the porous disc is directly related to the incoming velocity, by the thrust coefficient, and can thus be connected to the representative power output. The first requirement is fulfilled, allowing temporal measurements of the power output. The thrust force of the porous disc can be measured with a strain gage on the turbine tower, as will be discussed in the next paragraph. A number of prior experiments have used model turbines with rotating rotors.[7–10,12–14,17,18] However, a rotating wind turbine model is not readily feasible at such a small size, would make the entire set-up overly complicated and would lack the possibility of high frequency power output measurements, due to the significantly more complicated system dynamics. The working point of interest is the so-called region 2 in which a wind turbine is controlled to work at its optimal performance. The porous disc was designed to match the constant thrust coefficient of a wind turbine operating in this region, typically around $C_T = 0.75...0.85$. The porous disc model hereby matches also the second requirement[11] while a rotating wind turbine model would require an extra control system to adjust the tip speed ratio based on the incoming velocity, complicating the design even more. The final design of the porous disc is shown on Figure 1. The model has a diameter of 0.03m and is produced with a 3D printer out of ABS polymer. Figure 2 compares the measured mean stream wise velocity defect and stream wise turbulence intensity in the wake of the porous disc with results for rotating wind turbine models in the literature.[15,17,18] At only a distance of 3 diameters downstream we find already a nearly Gaussian mean velocity profile, typically associated with self similar axi-symmetrical wakes, characterizing the far wake of a wind turbine. Matching the mean velocity profile with the wake of a rotating wind turbine should result in similar turbulence intensity profiles for the far wake, where blade signatures are not visible any more due to turbulent mixing and where the turbulence is mainly governed by the velocity shear, confirmed for porous discs by measurements in Refs. [15–18]. Differences in the measured turbulence intensity profiles on Figure 2 (b) can be explained by the differences in background turbulence intensity and thrust coefficient between the two compared wind turbine models. It can be concluded that the designed porous disc model is capable of reproducing the far wake of a wind turbine in a turbulent flow with sufficient accuracy, hereby confirming that the second requirement is met. The designed porous disc hereby allows studying the power output of a wind farm.

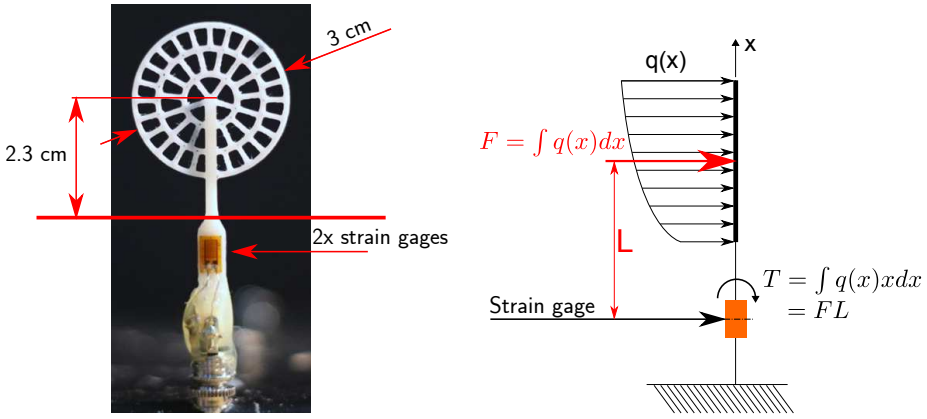

(a) (b)

Figure 1. (a) Photograph of the porous disc model. (b) Load distributions on the disc resulting in a torque measured by the strain gage.

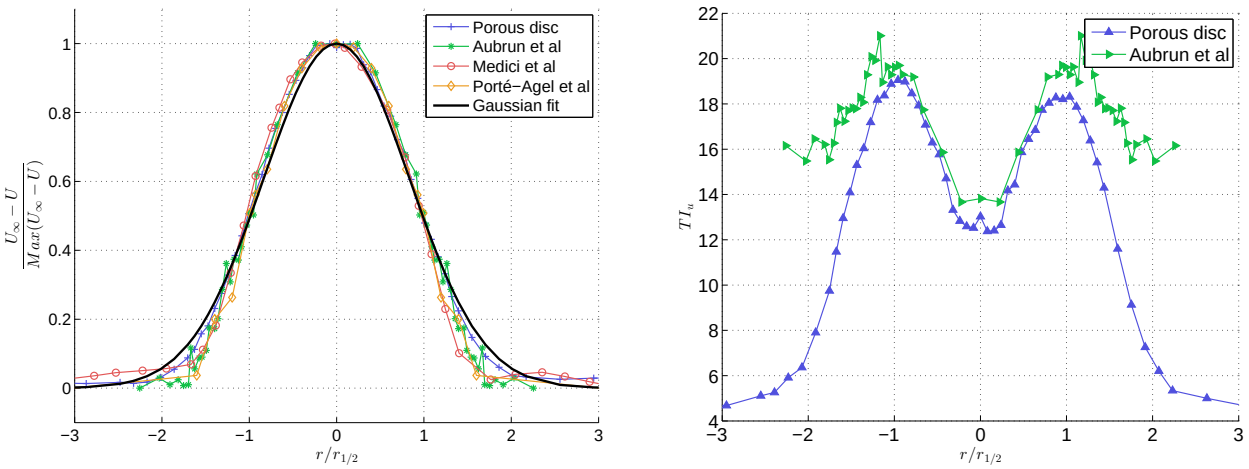

(a) (b)

Figure 2. Wake comparison of the porous disc model with several rotating wind turbine models in the literature, at a downstream distance of 3D. (a) Normalized mean velocity deficit. (b) Streamwise turbulence intensity.

Table 1. Characteristics of the rotating wind turbine models from the literature used for the comparison in Figure 2.

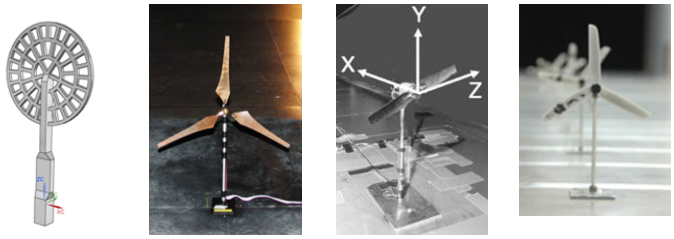

	Porous disc	Aubrun et al.	Medici et al.	Zhang et al
C_T	0.76 ± 0.04	0.5	0.84	0.42
Background turbulence intensity	5%	13%	4.5%	2%
Diameter	$0.03m$	$0.416m$	$0.18m$	$0.13m$
U_∞	$10m/s$	$2.5m/s$	$8.5m/s$	$2.5m/s$

II.B. Model instrumentation

The integrated thrust force on the porous disc is determined by measuring the bending of the turbine tower with a half-bridge strain gage apparatus. For constant material properties, the measured strain depends linearly on the resulting torque acting at the location of the strain gage, see Figure 1 (b). This torque can be found from the integration over the disk of the force distribution times the distance to the location of the strain gage. For symmetrical load distributions the torque equals the total thrust force times the distance to the center of the disc. For non-uniform load distributions however, the total representative thrust force will shift away from the center of the disc. Thanks to the cylindrical shape of the porous disc, which emphasizes the importance of the center, the shift in location is sufficiently small and can be expected to be 1% for a smooth wall boundary layer[19] (Type 1) and 6% for a very rough wall boundary layer flow[19] (Type 5). The systematic measurement error due to the incoming boundary layer profile in this measurement is estimated to be +4%. Turbines in the first row are corrected for this error. For the downstream located turbines we assume the flow to be well mixed due to the presence of the turbine wakes[9] , resulting in a much smaller load non-uniformity. The measurement error can be reduced in the design by increasing the distance between the center of the disc and the location of the strain gages. By modeling the structural response of the porous disc as a harmonic oscillator with one dominant natural frequency, the thrust force is calculated from the strain measurements. The spring and damping coefficient are determined for every turbine from a static and

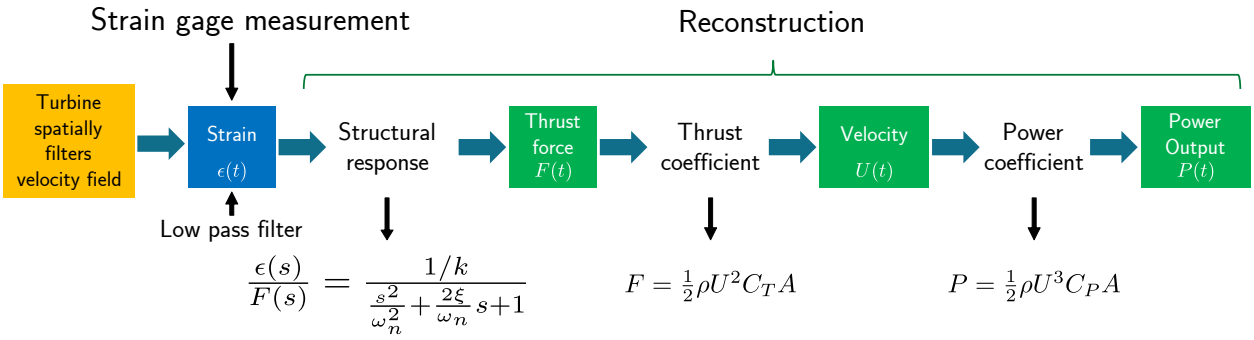

Figure 3. Reconstruction methodology to calculate the thrust force, velocity and power output from the measured strain signal. The structural response is modeled by the transfer function of a harmonic system with one significant natural frequency.

dynamic calibration. With the thrust coefficient we reconstruct the incoming spatially averaged velocity. The reconstructed velocity then allows to estimate the power of the model by assuming a realistic power coefficient. The reconstruction procedure is shown on Figure 3. For each of these signals we now have the time signal. The accuracy of the reconstruction scheme is verified by a simultaneous measurement with a

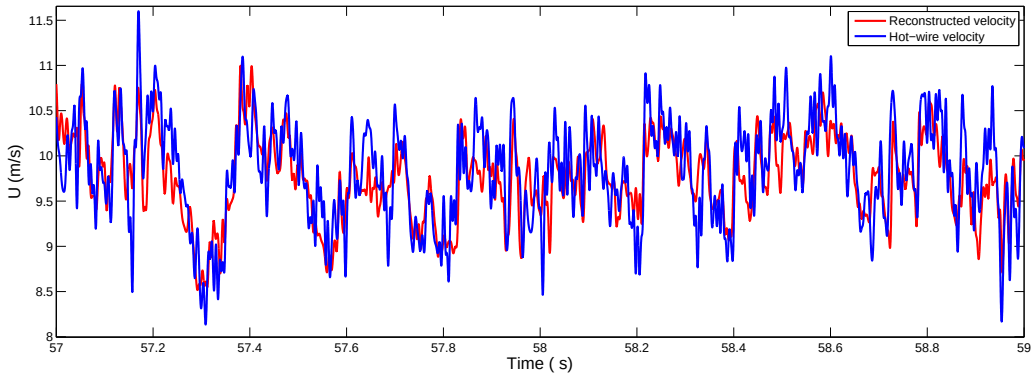

Figure 4. Comparison of the reconstructed velocity from the porous disc and the velocity from the hot - wire probe in time domain. Both signals are filtered at $f = 150Hz$. The correlation coefficient between both signals is $\rho = 0.73$.

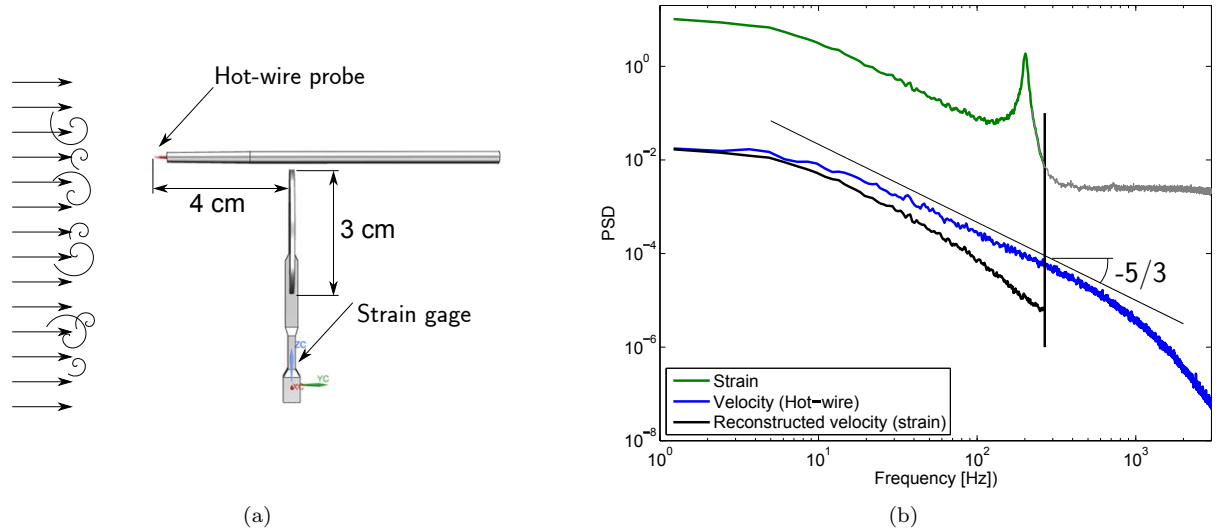

(a) (b)

Figure 5. (a) Measurement set-up for the reconstruction verification measurement. (b) Power spectrum density for the measured and reconstructed signals.

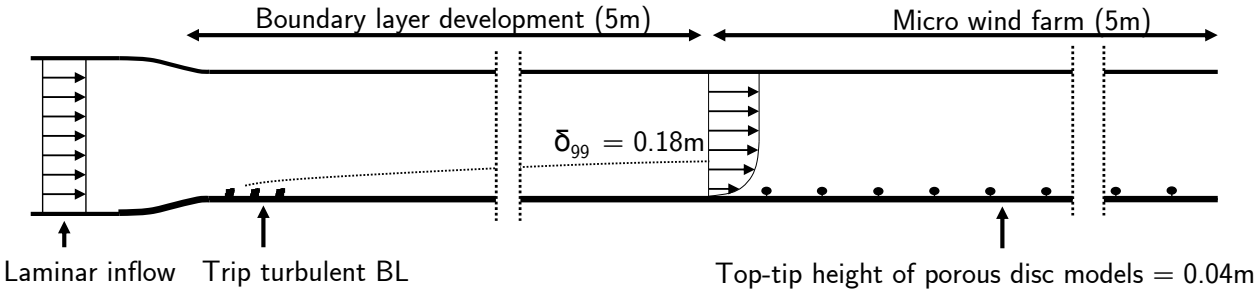

Figure 6. Schematic overview of the wind-tunnel test section.

hot-wire probe and a porous disc model in a uniform isotropically decaying turbulent flow. For comparisons, all signals have been filtered by a sharp cutoff filter with $f_c = 150Hz$. Figure 5 (a) shows the measurement set-up and Figure 4 a qualitative comparison of the time signal for the reconstructed velocity from the porous disc and the velocity from the hot-wire probe. Considering the difference in location and the spatial filtering of the porous disc, a good agreement is found between the two signals. The correlation factor is $\rho = 0.73$. Figure 5 compares the power spectrum of the reconstructed signals with the power spectrum of the measured velocity from the hot-wire probe. The power spectrum of the hot-wire velocity signal clearly shows the inertial and dissipation range. The strain gage signal from the porous disc shows a distinct peak due to the natural frequency of the model. With the structural response and thrust coefficient, the total thrust force and velocity are calculated. From the spectrum of the reconstructed velocity it can be concluded that the peak due to the natural frequency can be compensated quite effectively, increasing the frequency range for which the model can be used. There is still a clear difference between the spectrum of the reconstructed velocity and the spectrum of the velocity from the hot-wire measurement. This difference is expected to be a result of the spatial filtering by the porous disc. Attempts to analytically describe the spatial low pass filter from the velocity spectrum tensor and considering isotropic turbulence have failed in accurately describing the measured filter. The reason is expected to originate in the non-linear filter process of the thrust force and possible small scale interactions of the flow with the grid. In order to reconstruct the unfiltered spectrum of the incoming velocity a low pass filter can be fitted to the measured spatial filtering, as part of the model calibration. It is concluded that the reconstruction methodology is effective, allowing detailed temporal measurements of the thrust force, spatially averaged velocity and power of the porous disc models.

II.C. Wind farm set-up

Measurements were done in the Corrsin wind-tunnel at the Johns Hopkins University. The closed loop wind-tunnel has a test section of 0.9m × 1.2m and 10m long. A primary contraction-ratio of 25 : 1 and a second of 1.27 : 1 result in a low turbulence inflow at the beginning of the test-section with a background turbulence intensity $TI_u \approx 0.12\%$. Half of the wind-tunnel test section is used to naturally develop the boundary layer, after being tripped by chains at the entrance of the test section. The boundary layer has

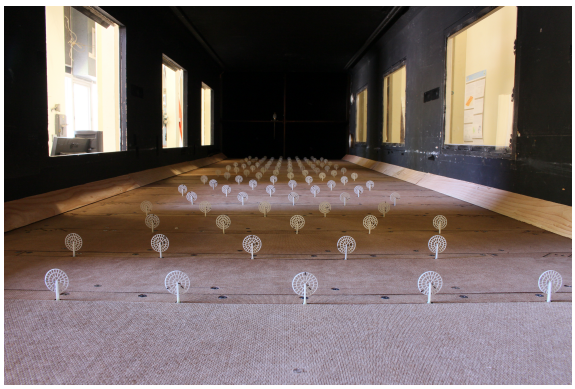

Figure 7. Photograph of the micro wind farm and set-up in the Corrsin wind tunnel.

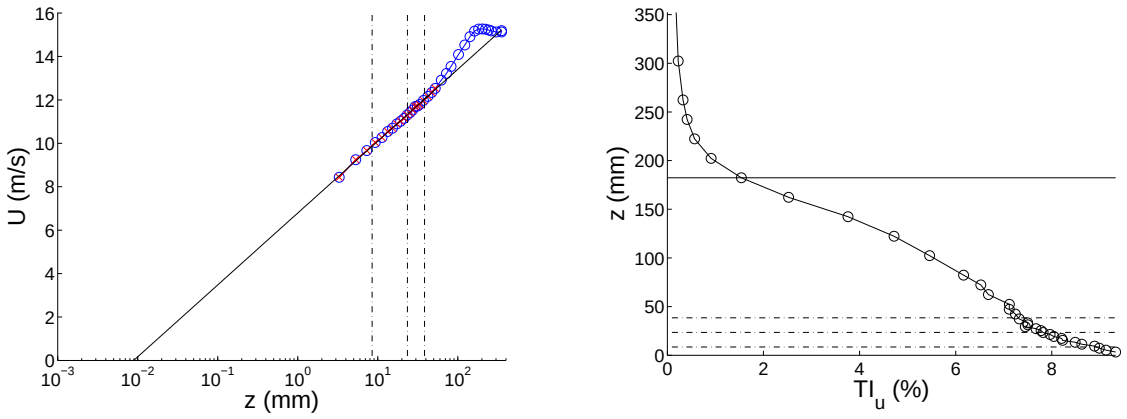

(a) (b)

Figure 8. (a) Measured velocity profile of the incoming boundary layer. (b) Measured streamwise turbulence intensity of the incoming boundary layer. Dashed lines represent the bottom-tip, hub and top-tip height of the porous disc model.

a height of $\delta_{99} = 0.18$m when it reaches the wind farm, this corresponds to 4.5 times the turbine top-tip height. Considering a scaling of $1:3,333$, the measured roughness height is $z_0 = 0.03m$ when scaled to full scale. This corresponds to a moderately rough boundary layer. Figure 8 shows the measured stream wise velocity and turbulence intensity when the flow reaches the wind farm. The turbine top-tip height is located in the log region of the flow. The stream wise turbulence intensity of the incoming boundary layer is around $7\% - 8\%$ at hub height. Measurements are done for a classical aligned wind farm with 100 porous disc models. (Figure 7) There are 20 rows and 5 columns with a stream wise spacing of $7D$ and a span wise spacing of $5D$.

III. Results and discussions

Figures 9-14 show the measurement results for the aligned wind farm. Data were acquired for the center columns 2,3 and 4. Table 2 gives an overview of the estimated measurement uncertainties. The reconstructed mean turbine velocity is shown on figure 9. As expected, a lower velocity is measured for the downstream turbines due to the wake effects of upstream turbines. Although the decrease in velocity with a stream wise spacing of 7D is only the order of $\approx 20\%$, it is seen from Figure 10 that the power decreases with $\approx 50\%$ for the downstream rows. This can be attributed to the cubic relation between power and velocity. It can be concluded that the designed wind farm measurement set-up is capable of measuring correctly the main trends in mean power. Figure 11 shows the stream wise turbulence intensity calculated from the reconstructed velocity signals of the porous disc models. This quantity is directly related to the turbine unsteady loading, where we focus on changes with a time scale larger than the time scale defined by the turbine diameter and the turbine velocity and larger than the natural frequency of the porous disc model. The natural frequency is the most restrictive ($f_n \approx 200Hz$) resulting in a smallest time scale the order of 20 seconds scaled to full scale conditions. (With a scaling factor of $1:3,333$.) Figure 11 shows an expected increase in turbulence intensity and turbine unsteady loading with increasing row number, which seems to level off near the end of the wind farm. Figure 12 makes further use of the detailed spatio-temporal information, captured by the measurement set-up, by showing the cross correlation between the power output of every porous disc with the center turbine in the first row. A strong correlation is found for the stream wise aligned turbines while the turbines from column 2 and 4 show the very low correlation in the span wise direction. This agrees with what we can expect from the directional characteristics of a typical boundary layer flow. These measurement results confirm the similar significant stream wise correlation found in a previous LES study[6] . Figures 13 and 14 show a time plot of the measured turbine power for a turbine in the first row, a turbine on row 15 and for the total wind farm. A higher skewness of the power signal is found for the turbine on row 15. Summation over all turbines reduces the power fluctuations and skewness significantly.

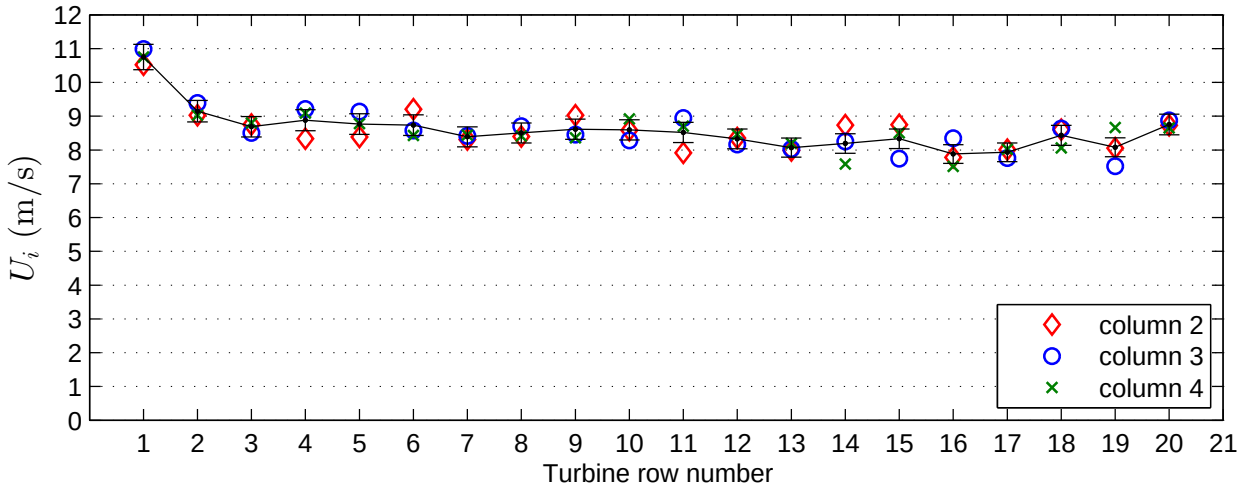

Figure 9. Reconstructed velocity from the porous disc models in the wind farm.

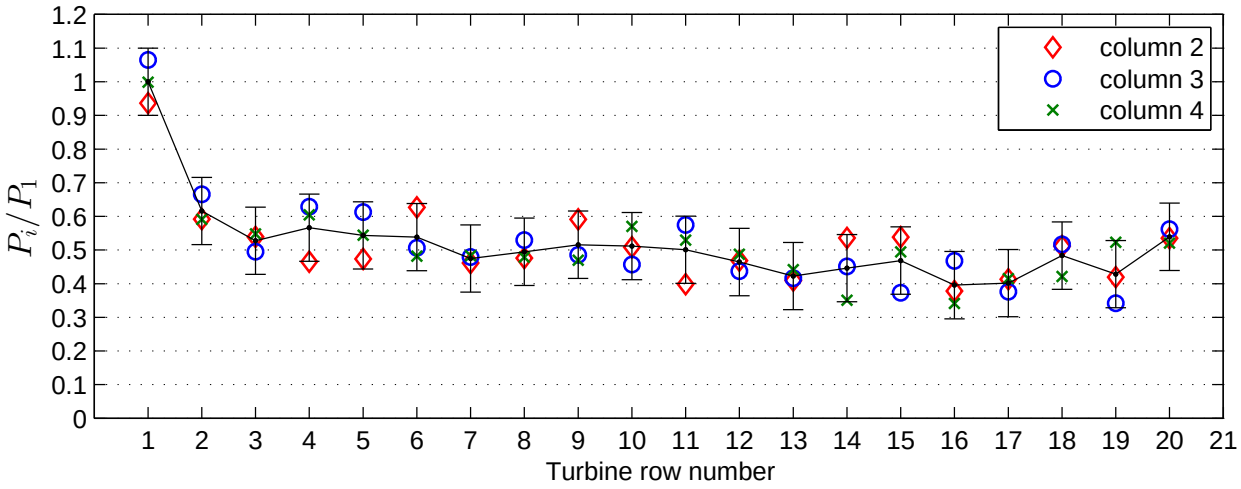

Figure 10. Reconstructed power from the porous disc models in the wind farm.

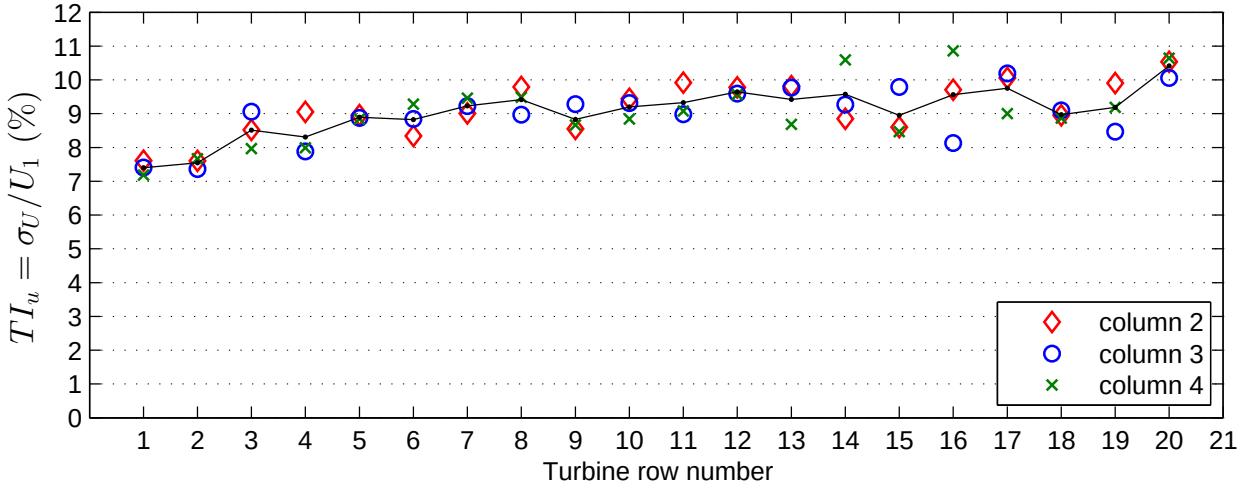

Figure 11. Turbulence intensity calculated from the reconstructed velocity from the porous disc models.

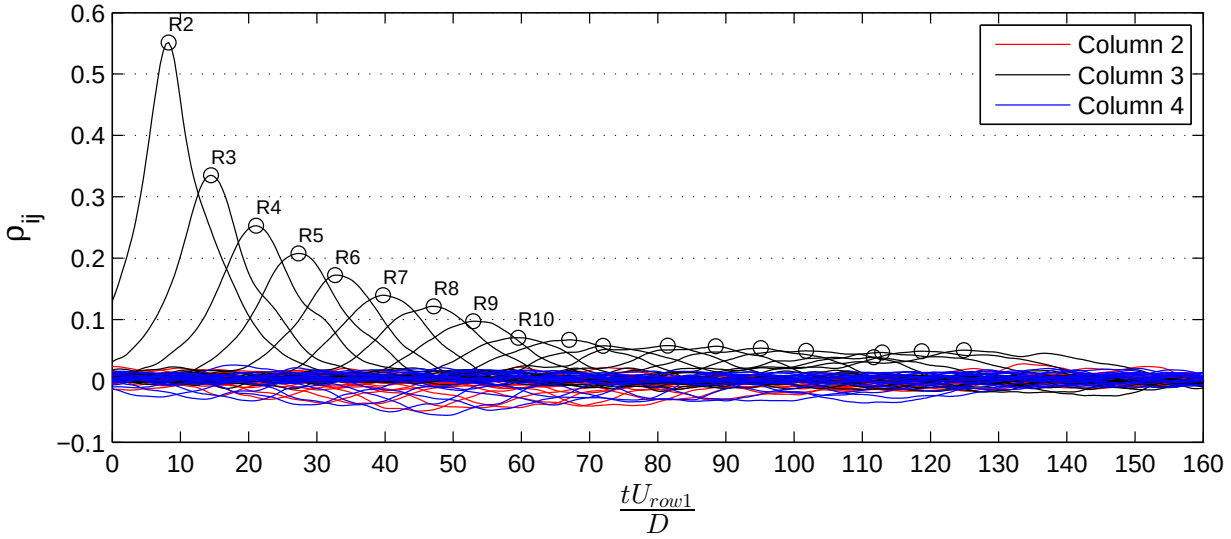

Figure 12. Cross correlation of all porous disc models with the center turbine in the first row, in function of the time delay. The time delay is nondimensionalized by the turbine diameter and mean velocity measured of the first row.

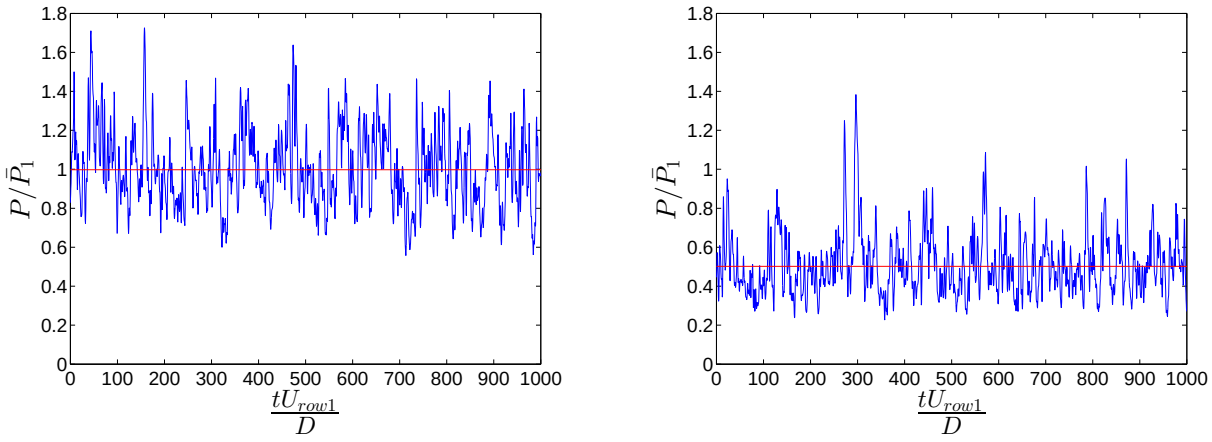

Figure 13. (a) Power signal for a turbine in the first row, with a skewness of 0.46. (b) The power signal of a turbine in row 15 shows a higher skewness of 0.92.

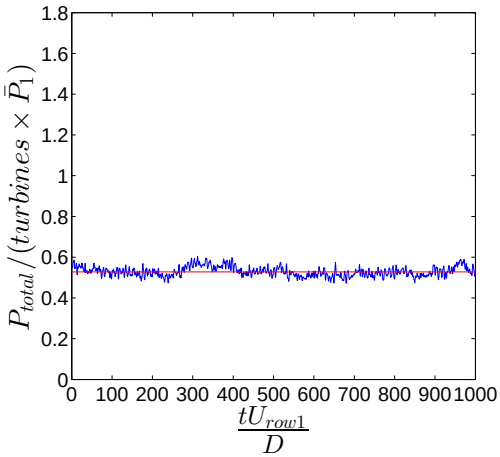

Figure 14. Total wind farm power normalized by total power when each turbine would be in the first row. The skewness of the power signal is 0.06.

Table 2. Measurement uncertainties estimated from a propagation analysis based on the strain measurement uncertainty and thrust coefficient uncertainty. Uncertainties are estimated relative to the smallest measured strain $\epsilon \approx 60\mu strain$. The highest measured strain is $\epsilon \approx 120\mu strain$ and the average strain over all wind turbines is $\epsilon \approx 73\mu strain$.

$\delta\epsilon$	$\pm 2\mu strain$
C_T	0.76 ± 0.04
$\delta F/F = \delta\epsilon/\epsilon$	$\pm 4\%$
$\delta U/U$	$\pm 3.5\%$
$\delta P/P$	$\pm 10\%$

IV. Conclusions

The mean power output, power output intermittency, unsteady loading and power output cross correlations were measured for an aligned wind farm with 100 wind turbine models in a wind-tunnel experiment. Instrumented porous disc models were used to represent the wind turbines and measure the quantities of interest with a high enough frequency response. The frequency response was limited by the natural frequency of the model. Translated to field conditions with a length-scale ratio of $1 : 3,333$, the frequencies available reach up to 0.06Hz. The measurement set-up is able to measure the main trends in mean row power. The increase in unsteady loading and turbulence intensity throughout the wind farm has been measured. A high correlation between the power output of stream wise aligned turbines has been confirmed by measurements, hereby demonstrating the detailed spatio-temporal information available from the measurements.

Acknowledgments

Work supported by ERC (ActiveWindFarms, grant no. 306471) and by NSF (WINDINSPIRE, grants CBET-113380 and IIA-1243482).

References

[1]Apt, J., "The spectrum of power from wind turbines," *Journal of Power Sources*, Vol. 169, No. 2, 2007, pp. 369 – 374.

[2]Meyers, J. and Meneveau, C., "Optimal turbine spacing in fully developed wind farm boundary layers," *Wind Energy*, Vol. 15, No. 2, 2012, pp. 305–317.

[3]Herbert-Acero, J. F., Probst, O., Rthor, P.-E., Larsen, G. C., and Castillo-Villar, K. K., "A Review of Methodological Approaches for the Design and Optimization of Wind Farms," *Energies*, Vol. 7, No. 11, 2014, pp. 6930.

[4]Goit, J. P. and Meyers, J., "Optimal control of energy extraction in wind-farm boundary layers," *Journal of Fluid Mechanics*, Vol. 768, 4 2015, pp. 5–50.

[5]De Rijcke, S., Driesen, J., and Meyers, J., "Power smoothing in large wind farms using optimal control of rotating kinetic energy reserves," *Wind Energy*, Vol. 18, No. 10, 2015, pp. 1777–1791.

[6]Stevens, R. J. A. M. and Meneveau, C., "Temporal structure of aggregate power fluctuations in large-eddy simulations of extended wind-farms," *Journal of Renewable and Sustainable Energy*, Vol. 6, No. 4, 2014.

[7]Milborrow, D., "The performance of arrays of wind turbines." *Journal of Industrial Aerodynamics*, Vol. 5, 1980, pp. 403–430.

[8]G. P. Corten, P. S. and Hegberg, T., "Turbine interaction in large offshore wind farms. Wind Tunnel Measurements." *ECN report ECN-C-04-048*, 2004.

[9]Chamorro, L. P. and Port-Agel, F., "Turbulent Flow Inside and Above a Wind Farm: A Wind-Tunnel Study," *Energies*, Vol. 4, No. 11, 2011, pp. 1916.

[10]Cal, R. B., Lebron, J., Castillo, L., Kang, H. S., and Meneveau, C., "Experimental study of the horizontally averaged flow structure in a model wind-turbine array boundary layer," *Journal of Renewable and Sustainable Energy*, Vol. 2, No. 1, 2010.

[11]Theunissen, R., Housley, P., Allen, C. B., and Carey, C., "Experimental verification of computational predictions in power generation variation with layout of offshore wind farms," *Wind Energy*, Vol. 18, No. 10, 2015, pp. 1739–1757, WE-13-0112.R3.

[12]Port-Agel, F., Lu, H., and Wu, Y.-T., "Interaction between Large Wind Farms and the Atmospheric Boundary Layer," *Procedia IUTAM*, Vol. 10, 2014, pp. 307 – 318, Mechanics for the World: Proceedings of the 23rd International Congress of Theoretical and Applied Mechanics, ICTAM2012.

[13]Chamorro, L. and Port-Agel, F., "A Wind-Tunnel Investigation of Wind-Turbine Wakes: Boundary-Layer Turbulence Effects," *Boundary-Layer Meteorology*, Vol. 132, No. 1, 2009, pp. 129–149.

[14]Jose Lebron, Raul Bayon Cal, H.-S. K. L. C. and Meneveau, C., "Interaction Between a Wind Turbine Array and a Turbulent Boundary Layer," *11th Americas Conference on Wind Engineering*, 2009.

[15]Aubrun, S., Loyer, S., Hancock, P., and Hayden, P., "Wind turbine wake properties: Comparison between a non-rotating

simplified wind turbine model and a rotating model," *Journal of Wind Engineering and Industrial Aerodynamics*, Vol. 120, 2013, pp. 1 – 8.

[16]Aubrun, S., Espaa, G., Loyer, S., Hayden, P., and Hancock, P., "Is the Actuator Disc Concept Sufficient to Model the Far-Wake of a Wind Turbine?" *Progress in Turbulence and Wind Energy IV*, edited by M. Oberlack, J. Peinke, A. Talamelli, L. Castillo, and M. Hlling, Vol. 141 of *Springer Proceedings in Physics*, Springer Berlin Heidelberg, 2012, pp. 227–230.

[17]Medici, D. and Alfredsson, P. H., "Measurements on a wind turbine wake: 3D effects and bluff body vortex shedding," *Wind Energy*, Vol. 9, No. 3, 2006, pp. 219–236.

[18]Zhang, W., Markfort, C., and Port-Agel, F., "Near-wake flow structure downwind of a wind turbine in a turbulent boundary layer," *Experiments in Fluids*, Vol. 52, No. 5, 2012, pp. 1219–1235.

[19]*Eurocode 1: Actions on structures - Part 1-4: General actions - Wind actions*, en 1991-1-4:2005+a1 ed.